CREEP DEFORMATIONS OF SHELLS OF REVOLUTION UNDER ASYMMETRICAL LOADING

S. TAKEZONO

Department of Mechanical Engineering,
Faculty of Engineering, Kumamoto University, Kumamoto 860, Japan

Y. WATANABE

Mitsubishi Heavy Industries, Ltd., Tokyo 100, Japan

SUMMARY

The paper describes the numerical analysis of creep deformations of shells of revolution under unsymmetrical loads with application to a cylindrical shell.

As a creep problem of shells of revolution is closely related to the analysis and the design of pressure vessels and pressure vessel components used in high temperature, there are many investigations on the creep of cylindrical shells, conical shells, spherical shells and so on. As to arbitrary shells of revolution, Penny presented the outline of a creep analysis of them and Takezono reported the numerical method of transient creep problems with applications to pressure vessel heads and to expansion bellows. These investigations, however, are almost all concerned with the case subjected to axisymmetrical loads, and few studies of the unsymmetrical problems are reported, in spite of importance of them in engineering.

In this paper the analytical formulation on the creep of axisymmetric shells undergoing unsymmetrical deformations is developed for two hardening laws: the time hardening law and the strain hardening law. The method is based on the creep power law, and on the assumption of plane stress condition and the Euler-Bernoulli hypothesis used in the ordinary thin shell theory. The basic differential equations derived for incremental values with respect to time are numerically solved by a finite difference method and the solutions at any time are obtained by integration of the incremental values. In conclusion the computer programs are developed which can be used to predict the creep deformations of arbitrary axisymmetrical shells.

As a numerical example the creep deformation of cylindrical shell of importance in practical use is treated, and the variations of displacements and internal forces with the lapse of time are discussed. The validity of the elastic solution from this method is confirmed by comparing with the solution by Budiansky and Radkowsky. The analysis of shells in steady creep becomes a subcase of the more general transient creep process described here.

1. Introduction

Since a creep problem of shells of revolution is closely related to the analysis and the design of pressure vessels and pressure vessel components used in high temperature, there are many investigations on the creep of spherical shells by Penny[1], conical shells by Cozzarelli[2], cylindrical shells by Cozzarelli[3], Penny[4], Byrne[5] and Murakami[6], and arbitrary shells of revolution by Penny[7],[8] and Takezono[9]-[12]. These investigations, however, are almost all concerned with the case subjected to axisymmetrical loads, and few studies of the unsymmetrical problems are reported except for Stern's[13], in spite of importance of them in engineering.

On the other hand the elastic analysis of unsymmetrical bending of shells of revolution has often been made as seen in the numerical method by Budiansky[14], by Kalnins[15], and so on. Although the creep behaviour is nonlinear with respect to time, the relations between the increments on each calculating stage may be regarded as linear. Therefore the fundamental relations between the increments can be solved by applying the method of elastic analysis.

In the present paper the numerical method of elastic analysis by Budiansky[14] is extended to deal with the creep problems. The method is based on the creep power law, and on the assumption of plane stress condition and the Kirchhoff-Love hypothesis used in the ordinary thin shell theory

As a numerical example the creep deformation of cylindrical shell subjected to asymmetrical end moments is analyzed, and the variations of displacements and internal forces with time are shown.

2. Analytical Formulations

2.1 Fundamental equations If the middle surface of axisymmetrical shells is given by $r=r(s)$, where r is the distance from the axis and s is the meridional distance measured from a boundary along the middle surface, as shown in Fig.1, the relations among the nondimensional carvatures $\omega_\xi(=a/R_\xi)$, $\omega_\theta(=a/R_\theta)$ and the nondimensional radius $\rho(=r/a)$ become as follows.

$$\left.\begin{array}{l} \omega_\xi=-(\gamma'+\gamma^2)/\omega_\theta, \quad \omega_\theta=\sqrt{1-(\rho')^2}/\rho \\ \omega_\theta'=\gamma(\omega_\xi-\omega_\theta), \quad \rho''/\rho=-\omega_\xi\omega_\theta \\ \gamma=\rho'/\rho, \quad \xi=s/a, \quad '=d/d\xi \end{array}\right\} \tag{1}$$

where a is the reference length.

Eliminating the transverse shear forces Q_ξ and Q_θ in the equilibrium equations in the Sanders theory[16] and differentiating with the time t the following equations are obtained.

$$\left.\begin{array}{l} a\left[\frac{\partial}{\partial\xi}(\rho\dot{N}_\xi)+\frac{\partial}{\partial\theta}(\dot{N}_{\xi\theta})-\rho'\dot{N}_\theta\right]+\omega_\xi\left[\frac{\partial}{\partial\xi}(\rho\dot{M}_\xi)+\frac{\partial}{\partial\theta}(\dot{M}_{\xi\theta})-\rho'\dot{M}_\theta\right]+\frac{1}{2}(\omega_\xi-\omega_\theta)\frac{\partial}{\partial\theta}(\dot{M}_{\xi\theta})+a^2p\dot{P}_\xi=0 \\ a\left[\frac{\partial}{\partial\theta}(\dot{N}_\theta)+\frac{\partial}{\partial\xi}(\rho\dot{N}_{\xi\theta})+\rho'\dot{N}_{\xi\theta}\right]+\omega_\theta\left[\frac{\partial}{\partial\theta}(\dot{M}_\theta)+\frac{\partial}{\partial\xi}(\rho\dot{M}_{\xi\theta})+\rho'\dot{M}_{\xi\theta}\right]+\frac{\rho}{2}\frac{\partial}{\partial\xi}[(\omega_\theta-\omega_\xi)\dot{M}_{\xi\theta}]+a^2\rho\dot{P}_\theta=0 \\ \frac{\partial}{\partial\xi}\left[\frac{\partial}{\partial\xi}(\rho\dot{M}_\xi)+\frac{\partial}{\partial\theta}(\dot{M}_{\xi\theta})-\rho'\dot{M}_\theta\right]+\frac{1}{\rho}\frac{\partial}{\partial\theta}\left[\frac{\partial}{\partial\theta}(\dot{M}_\theta)+\frac{\partial}{\partial\xi}(\rho\dot{M}_{\xi\theta})+\rho'\dot{M}_{\xi\theta}\right]-a\rho(\omega_\xi\dot{N}_\xi+\omega_\theta\dot{N}_\theta)+a^2\rho\dot{P}_\zeta=0 \end{array}\right\} \tag{2}$$

where

$$\dot{M}_{\xi\theta}=(\dot{M}_{\xi\theta}+\dot{M}_{\theta\xi})/2\,, \qquad \dot{N}_{\xi\theta}=(\dot{N}_{\xi\theta}+\dot{N}_{\theta\xi})/2+[(1/R_\theta)-(1/R_\xi)](\dot{M}_{\xi\theta}-\dot{M}_{\theta\xi})/4 \tag{3}$$

and the notations are shown in Fig. 2.

The membrane strains of the middle surface are given by

$$\dot{\varepsilon}_{\xi m}=\frac{1}{a}\frac{\partial}{\partial\xi}(\dot{U}_\xi)+\omega_\xi\dot{U}_\zeta\,, \qquad \dot{\varepsilon}_{\theta m}=\frac{1}{a}\left[\frac{1}{\rho}\frac{\partial}{\partial\theta}(\dot{U}_\theta)+\gamma\dot{U}_\xi+\omega_\theta\dot{U}_\zeta\right], \qquad \dot{\varepsilon}_{\xi\theta m}=\frac{1}{2a}\left[\frac{1}{\rho}\frac{\partial}{\partial\theta}(\dot{U}_\xi)+\frac{\partial}{\partial\xi}(\dot{U}_\theta)-\gamma\dot{U}_\theta\right] \tag{4}$$

where $\dot{\varepsilon}_{\xi\theta m}$ is half the usual engineering shear strain. Also the bending distortions are as follows.

$$\dot{\kappa}_\xi=\frac{1}{a}\frac{\partial\dot{\phi}_\xi}{\partial\xi},\quad \dot{\kappa}_\theta=\frac{1}{a}\left(\frac{1}{\rho}\frac{\partial\dot{\phi}_\theta}{\partial\theta}+r\dot{\phi}_\xi\right),\quad \dot{\kappa}_{\xi\theta}=\frac{1}{2a}\left\{\frac{1}{\rho}\frac{\partial\dot{\phi}_\xi}{\partial\theta}+\frac{\partial\dot{\phi}_\theta}{\partial\xi}-r\dot{\phi}_\theta+\frac{1}{2a}(\omega_\xi-\omega_\theta)\left(\frac{1}{\rho}\frac{\partial\dot{U}_\xi}{\partial\theta}-\frac{\partial\dot{U}_\theta}{\partial\xi}-\gamma\dot{U}_\theta\right)\right\} \tag{5}$$

where rotations $\dot{\phi}_\xi$ and $\dot{\phi}_\theta$ are

$$\dot{\phi}_\xi=\frac{1}{a}\left(-\frac{\partial\dot{U}_\zeta}{\partial\xi}+\omega_\xi\dot{U}_\xi\right),\quad \dot{\phi}_\theta=\frac{1}{a}\left(-\frac{1}{\rho}\frac{\partial\dot{U}_\zeta}{\partial\theta}+\omega_\theta\dot{U}_\theta\right) \tag{6}$$

Under the Kirchhoff-Love hypothesis and the neglect of terms of order ζ/R_ξ and ζ/R_θ relative to unity, the strains at the distance ζ from the middle surface, $\dot{\varepsilon}_\xi$, $\dot{\varepsilon}_\theta$, $\dot{\varepsilon}_{\xi\theta}$, are

$$\dot{\varepsilon}_\xi=\dot{\varepsilon}_{\xi m}+\zeta\dot{\kappa}_\xi,\quad \dot{\varepsilon}_\theta=\dot{\varepsilon}_{\theta m}+\zeta\dot{\kappa}_\theta,\quad \dot{\varepsilon}_{\xi\theta}=\dot{\varepsilon}_{\xi\theta m}+\zeta\dot{\kappa}_{\xi\theta} \tag{7}$$

respectively.

In the theory of creep it is assumed that in a given increment of time the total strain increments are composed of an elastic part and a part due to creep. Since the elastic strain rates are directly proportional to the stress rates by Hooke's law, the total strain rates may be expressed as follows.

$$\dot{\varepsilon}_\xi=\frac{1}{E}(\dot{\sigma}_\xi-\nu\dot{\sigma}_\theta)+\dot{\varepsilon}_{\xi c},\quad \dot{\varepsilon}_\theta=\frac{1}{E}(\dot{\sigma}_\theta-\nu\dot{\sigma}_\xi)+\dot{\varepsilon}_{\theta c},\quad \dot{\varepsilon}_{\xi\theta}=\frac{1+\nu}{E}\dot{\sigma}_{\xi\theta}+\dot{\varepsilon}_{\xi\theta c} \tag{8}$$

where $\dot{\varepsilon}_{\xi c}$, $\dot{\varepsilon}_{\theta c}$ and $\dot{\varepsilon}_{\xi\theta c}$ are the creep strain rates, and E and ν are Young's modulus and Poisson's ratio, respectively.

Now, if it is assumed that in the transient creep the creep strain in uni-axial state for constant stress may be given by

$$\varepsilon_c=A\sigma^n t^m \tag{9}$$

and eq.(9) is extended to the plane stress state assumed in the ordinary shell theory under the assumptions that the solid is isotropic, that the material obeys the Von Mises flow rule and that the creep strains are incompressible, then the components of creep strain rate, $\dot{\varepsilon}_{\xi c}$, $\dot{\varepsilon}_{\theta c}$ and $\dot{\varepsilon}_{\xi\theta c}$, may be written as follows for the time hardening and the strian hardening theories[17].

$$\dot{\varepsilon}_{\xi c}=(mA)\sigma_e^{n-1}t^{m-1}\left(\sigma_\xi-\frac{1}{2}\sigma_\theta\right),\quad \dot{\varepsilon}_{\theta c}=(mA)\sigma_e^{n-1}t^{m-1}\left(\sigma_\theta-\frac{1}{2}\sigma_\xi\right),\quad \dot{\varepsilon}_{\xi\theta c}=\left(\frac{3}{2}mA\right)\sigma_e^{n-1}t^{m-1}\sigma_{\xi\theta} \tag{10}$$

$$\dot{\varepsilon}_{\xi c}=(mA^{1/m})\sigma_e^{(n-m)/m}\varepsilon_{ec}^{(m-1)/m}\left(\sigma_\xi-\frac{1}{2}\sigma_\theta\right),\quad \dot{\varepsilon}_{\theta c}=(mA^{1/m})\sigma_e^{(n-m)/m}\varepsilon_{ec}^{(m-1)/m}\left(\sigma_\theta-\frac{1}{2}\sigma_\xi\right),\quad \dot{\varepsilon}_{\xi\theta c}=\left(\frac{3}{2}mA^{1/m}\right)\sigma_e^{(n-m)/m}\varepsilon_{ec}^{(m-1)/m}\sigma_{\xi\theta} \tag{11}$$

where

$$\sigma_e=\sqrt{\sigma_\xi^2+\sigma_\theta^2-\sigma_\xi\sigma_\theta+3\sigma_{\xi\theta}^2}\qquad \varepsilon_{ec}=\int_0^t\sqrt{\frac{4}{3}(\dot{\varepsilon}_{\xi c}^2+\dot{\varepsilon}_{\theta c}^2+\dot{\varepsilon}_{\xi c}\dot{\varepsilon}_{\theta c}+\dot{\varepsilon}_{\xi\theta c}^2)}\,dt \tag{12}$$

and A, n and m are obtained from a fit of uniaxial test data.

Substituting eqs.(7) into eqs.(8) and solving them about stresses, the stresses are

$$\dot{\sigma}_\xi=\frac{E}{1-\nu^2}\{\dot{\varepsilon}_{\xi m}+\nu\dot{\varepsilon}_{\theta m}+\zeta(\dot{\kappa}_\xi+\nu\dot{\kappa}_\theta)\}-\dot{\sigma}_{\xi c},\quad \dot{\sigma}_\theta=\frac{E}{1-\nu^2}\{\dot{\varepsilon}_{\theta m}+\nu\dot{\varepsilon}_{\xi m}+\zeta(\dot{\kappa}_\theta+\nu\dot{\kappa}_\xi)\}-\dot{\sigma}_{\theta c},\quad \dot{\sigma}_{\xi\theta}=\frac{E}{1+\nu}(\dot{\varepsilon}_{\xi\theta m}+\zeta\dot{\kappa}_{\xi\theta})-\dot{\sigma}_{\xi\theta c} \tag{13}$$

where

$$\dot{\sigma}_{\xi c}=\frac{E}{1-\nu^2}(\dot{\varepsilon}_{\xi c}+\nu\dot{\varepsilon}_{\theta c}),\quad \dot{\sigma}_{\theta c}=\frac{E}{1-\nu^2}(\dot{\varepsilon}_{\theta c}+\nu\dot{\varepsilon}_{\xi c}),\quad \dot{\sigma}_{\xi\theta c}=\frac{E}{1+\nu}\dot{\varepsilon}_{\xi\theta c} \tag{14}$$

From eqs.(13) the membrane forces and the resultant moments are as follows.

$$\left.\begin{aligned}&\dot{N}_\xi=\frac{Eh}{1-\nu^2}(\dot{\varepsilon}_{\xi m}+\nu\dot{\varepsilon}_{\theta m})-\dot{N}_{\xi c},\quad \dot{N}_\theta=\frac{Eh}{1-\nu^2}(\dot{\varepsilon}_{\theta m}+\nu\dot{\varepsilon}_{\xi m})-\dot{N}_{\theta c},\quad \dot{N}_{\xi\theta}=\frac{Eh}{1+\nu}\dot{\varepsilon}_{\xi\theta m}-\dot{N}_{\xi\theta c}\\&\dot{M}_\xi=\frac{Eh^3}{12(1-\nu^2)}(\dot{\kappa}_\xi+\nu\dot{\kappa}_\theta)-\dot{M}_{\xi c},\quad \dot{M}_\theta=\frac{Eh^3}{12(1-\nu^2)}(\dot{\kappa}_\theta+\nu\dot{\kappa}_\xi)-\dot{M}_{\theta c},\quad \dot{M}_{\xi\theta}=\frac{Eh^3}{12(1+\nu)}\dot{\kappa}_{\xi\theta}-\dot{M}_{\xi\theta c}\end{aligned}\right\} \tag{15}$$

where

$$\left.\begin{aligned}&\dot{N}_{\xi\epsilon}=\int_{-h/2}^{h/2}\dot{\sigma}_{\xi\epsilon}d\zeta,\quad \dot{N}_{\theta\epsilon}=\int_{-h/2}^{h/2}\dot{\sigma}_{\theta\epsilon}d\zeta,\quad \dot{N}_{\xi\theta\epsilon}=\int_{-h/2}^{h/2}\dot{\sigma}_{\xi\theta\epsilon}d\zeta\\&\dot{M}_{\xi\theta}=\int_{-h/2}^{h/2}\dot{\sigma}_{\xi\theta}\zeta d\zeta,\quad \dot{M}_{\theta\epsilon}=\int_{-h/2}^{h/2}\dot{\sigma}_{\theta\epsilon}\zeta d\zeta,\quad \dot{M}_{\xi\theta\epsilon}=\int_{-h/2}^{h/2}\dot{\sigma}_{\xi\theta\epsilon}\zeta d\zeta\end{aligned}\right\}\tag{16}$$

A complete set of field equations for the 29 independent variables: $\dot{N}_\xi, \dot{N}_\theta, \dot{N}_{\xi\theta}, \dot{M}_\xi, \dot{M}_\theta, \dot{M}_{\xi\theta}, \dot{U}_\xi, \dot{U}_\theta, \dot{U}_\zeta, \dot{\epsilon}_{\xi m}, \dot{\epsilon}_{\theta m}, \dot{\epsilon}_{\xi\theta m}, \dot{\kappa}_\xi, \dot{\kappa}_\theta, \dot{\kappa}_{\xi\theta}, \dot{\phi}_\xi, \dot{\phi}_\theta, \dot{\sigma}_\xi, \dot{\sigma}_\theta, \dot{\sigma}_{\xi\theta}, \dot{\sigma}_{\xi\epsilon}, \dot{\sigma}_{\theta\epsilon}, \dot{\sigma}_{\xi\theta\epsilon}, \dot{N}_{\xi\epsilon}, \dot{N}_{\theta\epsilon}, \dot{N}_{\xi\theta\epsilon}, \dot{M}_{\xi\epsilon}, \dot{M}_{\theta\epsilon}, \dot{M}_{\xi\theta\epsilon}$ now is given by the 29 equations, (2), (4)-(6) and (13)-(16)

2.2 Nondimensional equations The 29 independent variables now will be expanded into Fourier series. Let σ_0 be a reference stress level, and solutions of the field equations will be obtained in the following forms.

$$\left.\begin{aligned}&\dot{N}_\xi=\sigma_0 h\sum_{n=0}^{\infty}\dot{n}_\xi^{(n)}\cos n\theta,\quad \dot{N}_{\xi\epsilon}=\sigma_0 h\sum_{n=0}^{\infty}\dot{n}_{\xi\epsilon}^{(n)}\cos n\theta,\quad \dot{N}_\theta=\sigma_0 h\sum_{n=0}^{\infty}\dot{n}_\theta^{(n)}\cos n\theta\\&\dot{N}_{\theta\epsilon}=\sigma_0 h\sum_{n=0}^{\infty}\dot{n}_{\theta\epsilon}^{(n)}\cos n\theta,\quad \dot{N}_{\xi\theta}=\sigma_0 h\sum_{n=1}^{\infty}\dot{n}_{\xi\theta}^{(n)}\sin n\theta,\quad \dot{N}_{\xi\theta\epsilon}=\sigma_0 h\sum_{n=1}^{\infty}\dot{n}_{\xi\theta\epsilon}^{(n)}\sin n\theta\\&\dot{M}_\xi=\frac{\sigma_0 h^2}{a}\sum_{n=0}^{\infty}\dot{m}_\xi^{(n)}\cos n\theta,\quad \dot{M}_{\xi\epsilon}=\frac{\sigma_0 h^2}{a}\sum_{n=0}^{\infty}\dot{m}_{\xi\epsilon}^{(n)}\cos n\theta\\&\dot{M}_\theta=\frac{\sigma_0 h^2}{a}\sum_{n=0}^{\infty}\dot{m}_\theta^{(n)}\cos n\theta,\quad \dot{M}_{\theta\epsilon}=\frac{\sigma_0 h^2}{a}\sum_{n=0}^{\infty}\dot{m}_{\theta\epsilon}^{(n)}\cos n\theta\\&\dot{M}_{\xi\theta}=\frac{\sigma_0 h^2}{a}\sum_{n=1}^{\infty}\dot{m}_{\xi\theta}^{(n)}\sin n\theta,\quad \dot{M}_{\xi\theta\epsilon}=\frac{\sigma_0 h^2}{a}\sum_{n=1}^{\infty}\dot{m}_{\xi\theta\epsilon}^{(n)}\sin n\theta\end{aligned}\right\}\tag{17}$$

$$\left.\begin{aligned}&\dot{U}_\xi=\frac{a\sigma_0}{E}\sum_{n=0}^{\infty}\dot{u}_\xi^{(n)}\cos n\theta,\quad \dot{U}_\theta=\frac{a\sigma_0}{E}\sum_{n=1}^{\infty}\dot{u}_\theta^{(n)}\sin n\theta,\quad \dot{U}_\zeta=\frac{a\sigma_0}{E}\sum_{n=0}^{\infty}\dot{u}_\zeta^{(n)}\cos n\theta\\&\dot{\epsilon}_{\xi m}=\frac{\sigma_0}{E}\sum_{n=0}^{\infty}\dot{\epsilon}_{\xi m}^{(n)}\cos n\theta,\quad \dot{\epsilon}_{\theta m}=\frac{\sigma_0}{E}\sum_{n=0}^{\infty}\dot{\epsilon}_{\theta m}^{(n)}\cos n\theta,\quad \dot{\epsilon}_{\xi\theta m}=\frac{\sigma_0}{E}\sum_{n=1}^{\infty}\dot{\epsilon}_{\xi\theta m}^{(n)}\sin n\theta\\&\dot{\kappa}_\xi=\frac{\sigma_0}{aE}\sum_{n=0}^{\infty}\dot{k}_\xi^{(n)}\cos n\theta,\quad \dot{\kappa}_\theta=\frac{\sigma_0}{aE}\sum_{n=0}^{\infty}\dot{k}_\theta^{(n)}\cos n\theta,\quad \dot{\kappa}_{\xi\theta}=\frac{\sigma_0}{aE}\sum_{n=1}^{\infty}\dot{k}_{\xi\theta}^{(n)}\sin n\theta\\&\dot{\phi}_\xi=\frac{\sigma_0}{E}\sum_{n=0}^{\infty}\dot{\varphi}_\xi^{(n)}\cos n\theta,\quad \dot{\phi}_\theta=\frac{\sigma_0}{E}\sum_{n=1}^{\infty}\dot{\varphi}_\theta^{(n)}\sin n\theta\end{aligned}\right\}\tag{18}$$

$$\left.\begin{aligned}&\dot{\sigma}_\xi=\sigma_0\sum_{n=0}^{\infty}\dot{s}_\xi^{(n)}\cos n\theta,\quad \dot{\sigma}_{\xi\epsilon}=\sigma_0\sum_{n=0}^{\infty}\dot{s}_{\xi\epsilon}^{(n)}\cos n\theta,\quad \dot{\sigma}_\theta=\sigma_0\sum_{n=0}^{\infty}\dot{s}_\theta^{(n)}\cos n\theta\\&\dot{\sigma}_{\theta\epsilon}=\sigma_0\sum_{n=0}^{\infty}\dot{s}_{\theta\epsilon}^{(n)}\cos n\theta,\quad \dot{\sigma}_{\xi\theta}=\sigma_0\sum_{n=1}^{\infty}\dot{s}_{\xi\theta}^{(n)}\sin n\theta,\quad \dot{\sigma}_{\xi\theta\epsilon}=\sigma_0\sum_{n=1}^{\infty}\dot{s}_{\xi\theta\epsilon}^{(n)}\sin n\theta\end{aligned}\right\}\tag{19}$$

Also expanding the loads into Fourier series,

$$\dot{P}_\xi=\frac{\sigma_0 h}{a}\sum_{n=0}^{\infty}\dot{p}_\xi^{(n)}\cos n\theta,\quad \dot{P}_\theta=\frac{\sigma_0 h}{a}\sum_{n=1}^{\infty}\dot{p}_\theta^{(n)}\sin n\theta,\quad \dot{P}_\zeta=\frac{\sigma_0 h}{a}\sum_{n=0}^{\infty}\dot{p}_\zeta^{(n)}\cos n\theta\tag{20}$$

Substituting eqs.(17)-(20) into above 29 equations and eliminating appropriately the variables, the resultant set for $u_\xi^{(n)}$, $u_\theta^{(n)}$, $u_\zeta^{(n)}$ and $m_\xi^{(n)}$ then can be obtained as follows.

$$\left.\begin{aligned}&a_1\dot{u}_\xi''+a_2\dot{u}_\xi'+a_3\dot{u}_\xi+a_4\dot{u}_\theta'+a_5\dot{u}_\theta+a_6\dot{u}_\zeta'+a_7\dot{u}_\zeta+a_8\dot{m}_\xi'+a_9\dot{m}_\xi=C_1\\&a_{10}\dot{u}_\xi'+a_{11}\dot{u}_\xi+a_{12}\dot{u}_\theta''+a_{13}\dot{u}_\theta'+a_{14}\dot{u}_\theta+a_{15}\dot{u}_\zeta''+a_{16}\dot{u}_\zeta'+a_{17}\dot{u}_\zeta+a_{18}\dot{m}_\xi=C_2\\&a_{19}\dot{u}_\xi'+a_{20}\dot{u}_\xi+a_{21}\dot{u}_\theta''+a_{22}\dot{u}_\theta'+a_{23}\dot{u}_\theta+a_{24}\dot{u}_\zeta''+a_{25}\dot{u}_\zeta'+a_{26}\dot{u}_\zeta+a_{27}\dot{m}_\xi''+a_{28}\dot{m}_\xi'+a_{29}\dot{m}_\xi=C_3\\&a_{30}\dot{u}_\xi'+a_{31}\dot{u}_\xi+a_{32}\dot{u}_\theta+a_{33}\dot{u}_\zeta''+a_{34}\dot{u}_\zeta'+a_{35}\dot{u}_\zeta+a_{36}\dot{m}_\xi=C_4\end{aligned}\right\}\tag{21}$$

where the superscript (n) on Fourier coefficients will be omitted for convenience, $a_1\sim a_{36}$ are constants determined from the shell form and the materials[14], and $C_1\sim C_4$ are

$$\left.\begin{aligned}C_1=&-\dot{p}_\xi+\dot{n}_{\xi\epsilon}'+\gamma(\dot{n}_{\xi\epsilon}-\dot{n}_{\theta\epsilon})+\frac{n}{\rho}\dot{n}_{\xi\theta\epsilon}-\lambda^2\gamma\omega_\xi(\dot{m}_{\theta\epsilon}-\nu\dot{m}_{\xi\epsilon})+\frac{n\lambda^2}{2\rho}(3\omega_\xi-\omega_\theta)\dot{m}_{\xi\theta\epsilon}\\C_2=&-\dot{p}_\theta+\dot{n}_{\xi\theta\epsilon}'+2\gamma\dot{n}_{\xi\theta\epsilon}-\frac{n}{\rho}\dot{n}_{\theta\epsilon}+\frac{n\lambda^2\omega_\theta}{\rho}(\nu\dot{m}_{\xi\epsilon}-\dot{m}_{\theta\epsilon})\\&+\frac{1}{2}(3\omega_\theta-\omega_\xi)\lambda^2\dot{m}_{\xi\theta\epsilon}'+\frac{1}{2}\lambda^2(\gamma(3\omega_\theta+\omega_\xi)-\omega_\xi')\dot{m}_{\xi\theta\epsilon}\\C_3=&-\dot{p}_\zeta-\omega_\xi\dot{n}_{\xi\epsilon}-\omega_\theta\dot{n}_{\theta\epsilon}+\lambda^2\left(\omega_\xi\omega_\theta-\frac{n^2}{\rho^2}\right)(\dot{m}_{\theta\epsilon}-\nu\dot{m}_{\xi\epsilon})\\&-\gamma\lambda^2(\dot{m}_{\theta\epsilon}'-\nu\dot{m}_{\xi\epsilon}')+\frac{2n\lambda^2}{\rho}\dot{m}_{\xi\theta\epsilon}'+\frac{2\gamma n\lambda^2}{\rho}\dot{m}_{\xi\theta\epsilon},\quad C_4=\dot{m}_{\xi\epsilon},\quad \lambda=h/a\end{aligned}\right\}\tag{22}$$

Next, substituting eqs.(4) and (15) into eqs.(13), eqs.(13) may be expressed with the solutions $\dot{u}_\xi$, $\dot{u}_\theta$, $\dot{u}_c$ and $\dot{m}_\xi$ in eqs.(21) as follows.

$$\left.\begin{aligned}
\dot{s}_\xi &= b\Big[\dot{u}_\xi' + \nu\gamma\dot{u}_\xi + \frac{n}{\rho}\nu\dot{u}_\theta + (\omega_\xi + \nu\omega_\theta)\dot{u}_c + \frac{\zeta}{ad}\dot{m}_\xi + \frac{\zeta}{ad}\dot{m}_{\xi c}\Big] - \dot{s}_{\xi c} \\
\dot{s}_\theta &= b\Big[\nu\dot{u}_\xi' - \frac{\zeta\gamma(1-\nu^2)}{a}\dot{u}_c' + \gamma\Big\{1 + \frac{(1-\nu^2)\zeta\omega_\xi}{a}\Big\}\dot{u}_\xi + \frac{n}{\rho}\Big\{1 + \frac{(1-\nu^2)\omega_\theta\zeta}{a}\Big\}\dot{u}_\theta \\
&\quad + \Big\{\omega_\theta + \nu\omega_\xi + \frac{(1-\nu^2)n^2\zeta}{a\rho^2}\Big\}\dot{u}_c + \frac{\zeta\nu}{ad}\dot{m}_\xi + \frac{\zeta\nu}{ad}\dot{m}_{\xi c}\Big] - \dot{s}_{\theta c} \\
\dot{s}_{\xi\theta} &= b\Big[\frac{1-\nu}{2}\Big\{1 + \frac{\zeta}{2a}(3\omega_\theta - \omega_\xi)\Big\}\dot{u}_\theta' + (1-\nu)\frac{\zeta n}{a\rho}\dot{u}_c' + \frac{1-\nu}{2}\frac{n}{\rho}\Big\{-1 + \frac{(\omega_\theta - 3\omega_\xi)\zeta}{2a}\Big\}\dot{u}_\xi \\
&\quad + \frac{1-\nu}{2}\gamma\Big\{-1 + \frac{\zeta(\omega_\xi - 3\omega_\theta)}{2a}\Big\}\dot{u}_\theta - (1-\nu)\frac{n\gamma\zeta}{a\rho}\dot{u}_c\Big] - \dot{s}_{\xi\theta c}
\end{aligned}\right\} \qquad (23)$$

where $b = 1/(1-\nu^2)$, $d = 1/12(1-\nu^2)$

The rates of internal forces and stresses related to creep in eqs.(22) and (23) become the following by the use of eqs.(14), (16), (17) and (19).

$$\left.\begin{aligned}
&\sigma_0\sum_{n=0}^{\infty}\dot{n}_{\xi}^{(n)}\cos n\theta = \frac{E}{h}\frac{1}{1-\nu^2}\int_{-h/2}^{h/2}(\dot{\varepsilon}_{\xi c} + \nu\dot{\varepsilon}_{\theta c})d\zeta, \quad \sigma_0\sum_{n=0}^{\infty}\dot{n}_{\theta}^{(n)}\cos n\theta = \frac{E}{h}\frac{1}{1-\nu^2}\int_{-h/2}^{h/2}(\dot{\varepsilon}_{\theta c} + \nu\dot{\varepsilon}_{\xi c})d\zeta \\
&\sigma_0\sum_{n=1}^{\infty}\dot{n}_{\xi\theta}^{(n)}\sin n\theta = \frac{E}{h}\frac{1}{1+\nu}\int_{-h/2}^{h/2}\dot{\varepsilon}_{\xi\theta c}d\zeta, \quad \sigma_0\sum_{n=0}^{\infty}\dot{m}_{\xi}^{(n)}\cos n\theta = \frac{aE}{h^3}\frac{1}{1-\nu^2}\int_{-h/2}^{h/2}\zeta(\dot{\varepsilon}_{\xi c} + \nu\dot{\varepsilon}_{\theta c})d\zeta \\
&\sigma_0\sum_{n=0}^{\infty}\dot{m}_{\theta}^{(n)}\cos n\theta = \frac{aE}{h^3}\frac{1}{1-\nu^2}\int_{-h/2}^{h/2}\zeta(\dot{\varepsilon}_{\theta c} + \nu\dot{\varepsilon}_{\xi c})d\zeta, \quad \sigma_0\sum_{n=1}^{\infty}\dot{m}_{\xi\theta}^{(n)}\sin n\theta = \frac{aE}{h^3}\frac{1}{1+\nu}\int_{-h/2}^{h/2}\zeta\dot{\varepsilon}_{\xi\theta c}d\zeta
\end{aligned}\right\} \qquad (24)$$

$$\sigma_0\sum_{n=0}^{\infty}\dot{s}_{\xi c}^{(n)}\cos n\theta = \frac{E}{1-\nu^2}(\dot{\varepsilon}_{\xi c} + \nu\dot{\varepsilon}_{\theta c}), \qquad \sigma_0\sum_{n=0}^{\infty}\dot{s}_{\theta c}^{(n)}\cos n\theta = \frac{E}{1-\nu^2}(\dot{\varepsilon}_{\theta c} + \nu\dot{\varepsilon}_{\xi c}), \qquad \sigma_0\sum_{n=1}^{\infty}\dot{s}_{\xi\theta c}^{(n)}\sin n\theta = \frac{E}{1+\nu}\dot{\varepsilon}_{\xi\theta c} \qquad (25)$$

The creep strain rates in right hand sides can be related to stresses by eqs.(10) or (11).

2.3 Boundary conditions and junction conditions When the values of the solutions in eqs. (21) are not given at boundaries of shells, i.e. $\dot{n}_\xi$, $\dot{n}_{\xi\theta}$, $\dot{q}_\xi$, $\dot{\psi}_\xi$ (Fig.1) are prescribed, they must be rewrite by the solutions as follows[12].

$$\left.\begin{aligned}
\dot{n}_\xi &= b_1\dot{u}_\xi' + b_2\dot{u}_\xi + b_3\dot{u}_\theta + b_4\dot{u}_c + d_1 \\
\dot{n}_{\xi\theta} &= b_5\dot{u}_\xi + b_6\dot{u}_\theta' + b_7\dot{u}_\theta + b_8\dot{u}_c' + b_9\dot{u}_c + d_2 \\
\dot{q}_\xi &= b_{10}\dot{u}_\xi + b_{11}\dot{u}_\theta' + b_{12}\dot{u}_\theta + b_{13}\dot{u}_c' + b_{14}\dot{u}_c + b_{15}\dot{m}_\xi' + b_{16}\dot{m}_\xi + d_3 \\
\dot{\psi}_\xi &= -\dot{u}_c' + \omega_\xi\dot{u}_\xi
\end{aligned}\right\} \qquad (26)$$

where $b_1 \sim b_{16}$ are the constants determined from the shell geometries and the materials, and $d_1 \sim d_3$ are

$$d_1 = -\dot{n}_{\xi c}, \quad d_2 = -\dot{n}_{\xi\theta c} - \frac{\lambda^2}{2}(3\omega_\theta - \omega_\xi)\dot{m}_{\xi\theta c}, \quad d_3 = \gamma\lambda^2\dot{m}_{\theta c} - \lambda^2\gamma\nu\dot{m}_{\xi c} - \frac{2n\lambda^2}{\rho}\dot{m}_{\xi\theta c} \qquad (27)$$

The differential equations (21) are not valid at points in the shell where discontinuities in geometry and / or mechanical property of the material exist. Accordingly, at such points equations of junction will be required which relate solution and its derivative on either side of a discontinuity. With plus and minus superscripts denoting values just beyond and ahead of a discontinuity, respectively, the conditions of geometrical compatibility are

$$\dot{u}_\xi^+ = \dot{u}_\xi^-, \quad \dot{u}_\theta^+ = \dot{u}_\theta^-, \quad \dot{u}_c^+ = \dot{u}_c^-, \quad \dot{\psi}_\xi^+ = \dot{\psi}_\xi^- \qquad (28)$$

and equilibrium requires that

$$\dot{n}_\xi^+ = \dot{n}_\xi^-, \quad \dot{n}_{\xi\theta}^+ = \dot{n}_{\xi\theta}^-, \quad \dot{q}_\xi^+ = \dot{q}_\xi^-, \quad \dot{m}_\xi^+ = \dot{m}_\xi^- \qquad (29)$$

The differential equations (21), the boundary conditions (26) and the junction conditions (28), (29) will be cast into a unified set of appropriate finite difference equations.

3. Numerical method

Suppose that p discontinuity locations $s_1, s_2 \cdots s_p$ occur in the range $(0, \bar{s})$ of the shell as shown in Fig.1, let the regions $(0, s_1)$, $(s_1, s_2), \cdots (s_p, \bar{s})$ be subdivided into N_1-1, $N_2-1, \cdots N_{p+1}-1$ eaual segments, respectively, and give the endpoints of the segments two indices, running from 1 at $s=0$ to $N(=\sum_{i=0}^{p+1} N_i)$ at $s=\bar{s}$, then the increments in the nondimensional variable ξ are

$$\left.\begin{aligned} \Delta_1 &= s_1/a(N_1-1) \\ \Delta_2 &= (s_2-s_1)/a(N_2-1) \\ &\vdots \\ \Delta_{p+1} &= (\bar{s}-s_p)/a(N_{p+1}-1) \end{aligned}\right\} \tag{30}$$

in the successive regions bounded by discontinuities.

The differential equations (21) are written in finite difference form at all stations except the discontinuity stations and the boundaries ($j=1, N$) on the basis of the usual central difference formulas:

$$\dot{Z}_j' = \frac{\dot{Z}_{j+1}-\dot{Z}_{j-1}}{2\Delta}, \quad \dot{Z}_j'' = \frac{\dot{Z}_{j+1}-2\dot{Z}_j+\dot{Z}_{j-1}}{\Delta^2} \tag{31}$$

where $\dot{Z}^T = \{\dot{u}_\xi, \dot{u}_\theta, \dot{u}_\zeta, \dot{m}_\xi\}$

For the boundary points ($j=1, N$) and discontinity points (e.g. $j=m$, $m+1$)

$$\left.\begin{aligned} \dot{Z}_1' &= \frac{-3\dot{Z}_1+4\dot{Z}_2-\dot{Z}_3}{2\Delta_1}, \quad \dot{Z}_n' = \frac{3\dot{Z}_n-4\dot{Z}_{n-1}+\dot{Z}_{n-2}}{2\Delta_n} \\ \dot{Z}_m' &= \frac{3\dot{Z}_m-4\dot{Z}_{m-1}+\dot{Z}_{m-2}}{2\Delta^-}, \quad \dot{Z}_{m+1}' = \frac{-3\dot{Z}_{m+1}+4\dot{Z}_{m+2}-\dot{Z}_{m+3}}{2\Delta^+} \end{aligned}\right\} \tag{32}$$

are employed. Where Δ^- and Δ^+ are the intervals ahead and beyond the station $j=m$, respectively.

Applying above difference formulas for the fundamental equations, the boundary ones and the junction ones, the following simultaneous equations with N unknowns respect to Z_j may be obtained.

$$A_j\dot{Z}_{j-1}+B_j\dot{Z}_j+C_j\dot{Z}_{j+1}=D_j \tag{33}$$

$$\left.\begin{aligned} &(AM)_m\dot{Z}_{m-2}+(BM)_m\dot{Z}_{m-1}+(CM)_m\dot{Z}_m+(DM)_{m+1}\dot{Z}_{m+1}+(EM)_{m+1}\dot{Z}_{m+2}+(FM)_{m+1}\dot{Z}_{m+3}=0 \\ &(GM)_m\dot{Z}_{m-2}+(HM)_m\dot{Z}_{m-1}+(IM)_m\dot{Z}_m+(JM)_{m+1}\dot{Z}_{m+1}+(KM)_{m+1}\dot{Z}_{m-2}+(LM)_{m+1}\dot{Z}_{m+3}=(SM)_m-(SM)_{m+1} \end{aligned}\right\} \tag{34}$$

$$\left.\begin{aligned} &(A1)\dot{Z}_1+(B1)\dot{Z}_2+(C1)\dot{Z}_3=(D1) \\ &(AN)\dot{Z}_{n-2}+(BN)\dot{Z}_{n-1}+(CN)\dot{Z}_n=(DN) \end{aligned}\right\} \tag{35}$$

Now, the above numerical method is concerned with the handling of the spatial aspect of the problem. However, in transient creep the temporal aspect also must be considered. The latter is usually handled with an incremental procedure. Thus, the numerical solution in a transient creep of shells of revolution proceeds as follows.

Step 1 : Determine the elastic solution in the shell by removing the dots and droping the terms of creep in eqs.(33)-(35).

Step 2 : Assume that the stresses obtained in Step 1 remain constant over a very small initial increment of time Δt_0 and calculate the increments of creep strains that occur in the incremental time Δt_0 by the use of the time hardening law, eqs.(10). Next by substitution of the increments of creep strains into the right hand side of eqs.(24) and expansion of them into Fourier series, obtain the values of $\dot{m}_{\xi c}^{(n)} \sim \dot{m}_{\xi\theta c}^{(n)}$, and calculate the incremental values during this incremental time Δt_0 by the use of eqs.(33)-(35). By adding these incremental values to the elastic solutions obtain the stresses and the displacements at $t=\Delta t_0$ for the time hardening law. Equations (24) are integrated numerically by dividing the thickness h of the shell into ten and employing Simpson's 1/3 rule. The number of terms

in Fourier series and Δt_0 value are chosen from consideration of the convergency of the solutions. In the initial routine eqs.(10) are employed for both the calculations based on the time hardening law and the strain hardening law.

Step 3 : Choose a suitable increment of time Δt . The time increment Δt is controlled as in each calculating step the increments of the internal force which varies remarkably with time become $1/\beta$ of initial elastic value at the point where the elastic value is maximum. The values of β in calculation may be decided from consideration of the convergency of the solutions.

Step 4 : Calculate the increments of stresses and displacements for Δt by introducing the stress values obtained in Step 2 into eqs.(10) or (11). By adding the increments of the stresses and the displacements for Δt to the results in Step 2 determine the stresses and the displacements at the end of the interval Δt. In this step the same numerical method as in Step 2 is employed.

Step 5 : Repeat Steps 3 and 4. Continue in this manner until a desired time interval has been achieved or until a steady state has been reached whichever occurs first.

4. Numerical example

As a numerical example of creep deformations of axisymmetrical shells under unsymmetrical loading the cylindrical shell subjected to asymmetrical end moments as shown in Fig.3 is treated.

The geometrical parameters of this shell are as follows.

$$\Delta=\frac{l}{2R(N-1)},\quad \rho=1,\quad \rho'=0,\quad \gamma=0,\qquad \omega_\theta=1,\quad \omega_\xi=\omega_\xi'=0 \tag{36}$$

Boundary conditions at the point A ($j=1$) and B ($j=N$) are respectively

$$t=0:\dot{U}_\xi=\dot{U}_\zeta'=\dot{M}_\xi'=\dot{N}_{\xi\theta}=0,\qquad t>0:\dot{U}_\xi=\dot{U}_\zeta'=\dot{M}_\xi'=\dot{N}_{\xi\theta}=0 \tag{37}$$

and

$$t=0:M_\xi=\alpha\cos 2\theta,\quad U_\xi=U_\theta=U_\zeta=0,\qquad t>0:\dot{M}_\xi=0,\quad \dot{U}_\xi=\dot{U}_\theta=\dot{U}_\zeta=0 \tag{38}$$

They are rewritten in the following nondimensional forms, where $\sigma_0=1$

$$t\geqq 0:\dot{u}_\xi^{(n)}=\dot{u}_\zeta'^{(n)}=\dot{m}_\xi'^{(n)}=0,\qquad \dot{n}_{\xi\theta}^{(n)}=b_5\dot{u}_\xi^{(n)}+b_6\dot{u}_\theta'^{(n)}+b_8\dot{u}_\zeta^{(n)}+d_2=0 \tag{39}$$

(The dots are dropped when $t=0$),

and

$$t=0:m_\xi^{(2)}=\alpha R/\sigma_0 h^2,\qquad m_\xi^{(n)}=0\ (n\neq 2),\quad u_\xi^{(n)}=u_\theta^{(n)}=u_\zeta^{(n)}=0,\qquad t>0:\dot{m}_\xi^{(n)}=\dot{u}_\xi^{(n)}=\dot{u}_\theta^{(n)}=\dot{u}_\zeta^{(n)}=0 \tag{40}$$

The material constants employed in calculations are

$$E=17\,000\ \mathrm{kg/mm^2},\quad \nu=0.3,\quad A=3.13\times 10^{-8}(\mathrm{kg/mm^2})^{-n}\mathrm{h}^{-m},\quad n=4.17,\quad m=0.166. \tag{41}$$

The values of constants correspond to 0.19 % carbon steel at 450°C. Figure 4 shows the creep curve of the material.

It is found from the calculations for various values of N that the difference between the elastic solutions for N=26 and 51 is about 1 %, and the difference between ones for N=51 and N=151 is about 0.3 %. Therefore N=51 is employed in the further creep analysis considering the capacity of the computer and the computing time.

It is seen from examination of the convergency of solutions with the number of terms of Fourier series [=(n + 1)/2] that the solutions are unstable when n = 5-9, but when $n \geq 11$ become stable and the difference between the solutions for n = 19 and 23 is less than 0.1 %. Accordingly in the further numerical calculations the authors employ n = 19

from the above-mentioned reason.

The other parameters related to the convergency of the solutions are determined as $\beta = 60$ and $\Delta\varepsilon_0 = 10^{-10}$.

Some of the essential features of the creep solutions from the time hardening law are shown in Figs.5-10. The solutions based on the strain hardening law scarcely differ from them.

5. Conclusions

In the paper the authors described the numerical analysis on creep deformations of shells of revolution under arbitrary loads with application to a cylindrical shell. The increments of all pertinent variables were expanded into Fourier series in the circumferential direction and decoupled sets of ordinary differential equations were solved by usual finite difference forms. The solutions at any time were obtained by integration of the incremental values.

In conclusion the computer programs were developed which could be used to predict the creep deformations of axisymmetrical shells under arbitrary loads.

As a numerical example the creep deformation of cylindrical shell of importance in practical use was discussed. The analysis of shell in steady creep becomes a subcase of the more general transient creep process described here.

References

[1] PENNY, R.K., "Creep of Spherical Shells Containing Discontinuity", Int. J. Mech. Sci., 9, 373 (1967).

[2] COZZARELLI, F.A., VITO, R.P., "Creep of Conical Membrane Shells under Aerodynamic Heating and Loading", AIAA J., 7, 412 (1969).

[3] COZZARELLI, F.A., PATEL, S.A., VENKATRAMAM, B., "Creep Analysis of Circular Cylindrical Shells", AIAA J., 3, 1298 (1965).

[4] PENNY, R.K., "Creep of Pressurised Cylindrical Shells", J. of Roy. Aero. Soc. 73, 514 (1969).

[5] BYRNE, T.P., MACKENZIE, A.C., "Secondary Creep of a Cylindrical Thin Shell Subject to Axisymmetric Loading", J. Mech. Engng. Sci., 8, 215 (1966).

[6] MURAKAMI, S., IWATSUKI, S., "Transient Creep of Circular Cylindrical Shells", Int. J. Mech. Sci., 11, 897 (1969).

[7] PENNY, R.K., "Axisymmetric Bending of the General Shell of Revolution during Creep", J. Mech. Engng. Sci., 6, 44 (1964).

[8] PENNY, R.K., "The Creep of Shells", Creep in Structures, 276 (1972), Springer-Verlag.

[9] TAKEZONO, S., TANAKA, K., NAKATSUKASA, M., "Transient Creep of Shells of Revolution", Bull. JSME, 16, 171 (1973).

[10] TAKEZONO, S., NAKATSUKASA, M., "Large Creep Deformations of Thin Shells of Revolution", Second Intl. Conf. on Structural Mechanics in Reactor Technology, Berlin, Germany (September 10-14, 1973).

[11] TAKEZONO. S., NAKATSUKASA,M., USUI, M., "Large Creep Deformations of Thin Shells of Revolution", Bull. JSME, 17, 888 (1974).

[12] TAKEZONO, S., TANAKA, T., "Numerical Analysis of Unsymmetrical Bending of Visco-Elastic Shells of Revolution", Bull. JSME, 17, 1397 (1974).

[13] STERN, G.S., "Creep Bending of Rotational Shell Structures Subject to Nonsymmetric Loads", Ph. D. Thesis, Univ. Calif., (1964).

[14] BUDIANSKY, F., RADKOWSKY, P.P., "Numerical Analysis of Unsymmetrical Bending of Shells of Revolution", AIAA J., 1, 1833 (1963).

[15] KALNINS, A., "Analysis of Shells of Revolution Subjected to Symmetrical and Nonsymmetrical Loads", Trans. ASME, Ser. E, 31 467 (1964).

[16] SANDERS, J.L.Jr., "An Improved First-Approximation Theory for Thin Shells", NASA Tech. Rep., R-24 (1959).

[17] FINNIE, I., HELLER, W.R., "Creep of Engineering Materials", (1959), McGraw-Hill.

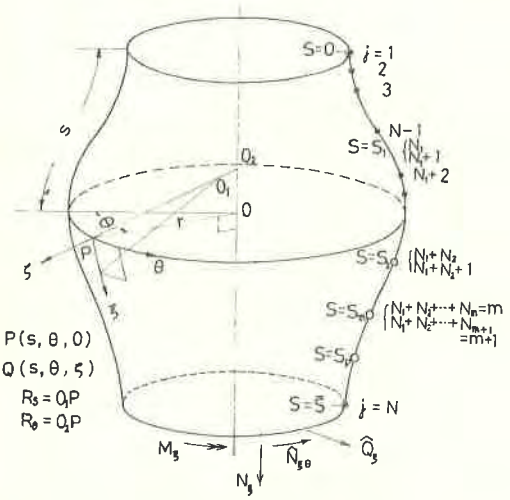

Fig. 1 Geometry and mesh points

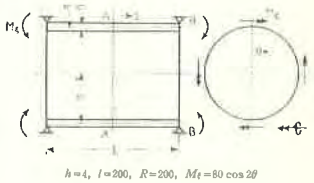

Fig. 3 Cylindrical shell

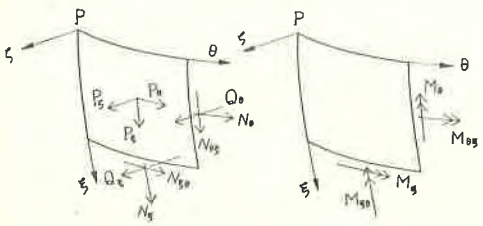

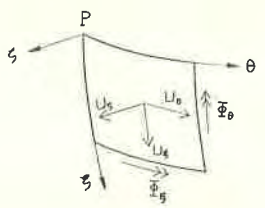

Fig. 2 Notations

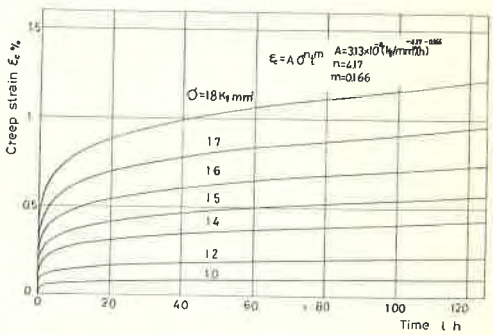

Fig. 4 Creep curves of material

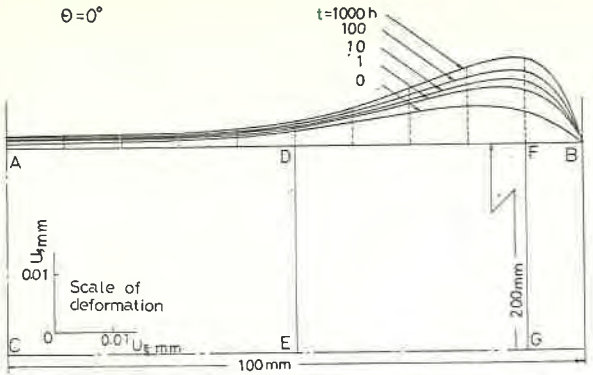

Fig. 5 Deformations in meridional section with time

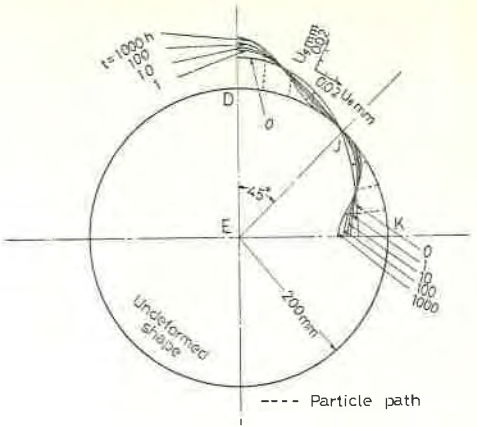

(b) ξ= 0.25

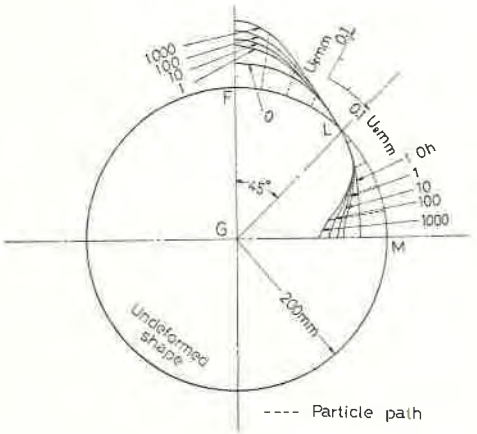

(a) ξ= 0.45

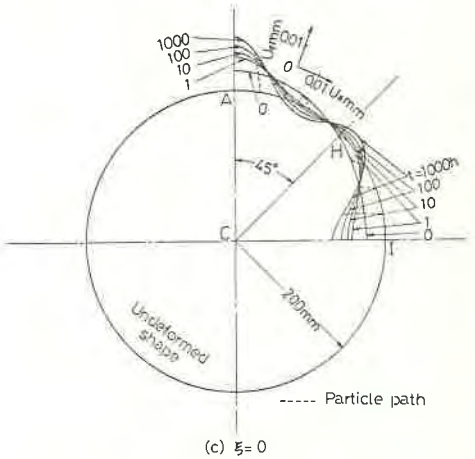

(c) ξ= 0

Fig. 6 Deformations in cross sections with time

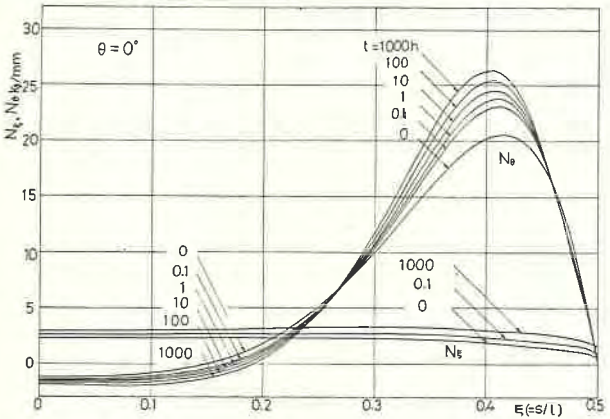

(a) N_ξ, N_θ

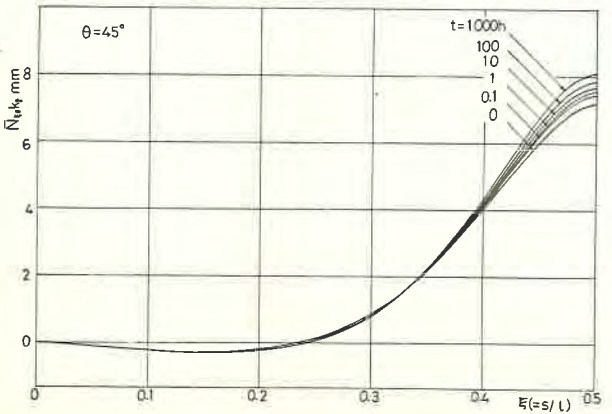

(b) $\bar{N}_{s\theta}$

Fig. 7 Variations of membrane forces with time

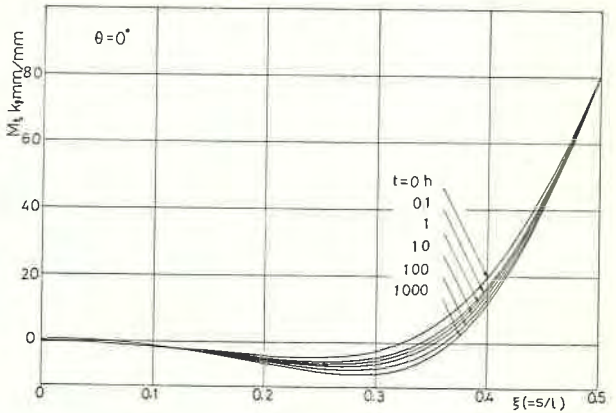

(a) M_ξ

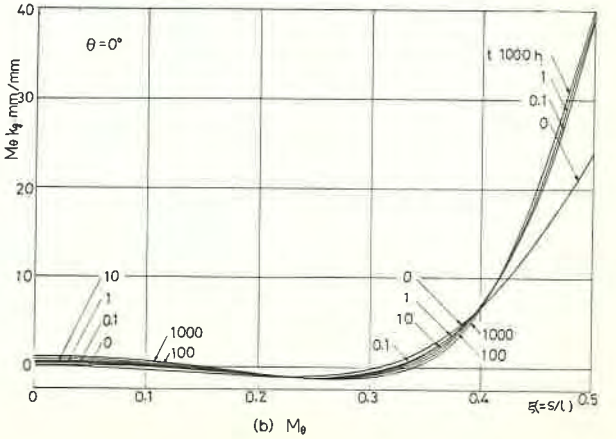

(b) M_θ

Fig. 8 Variations of resultant moments with time

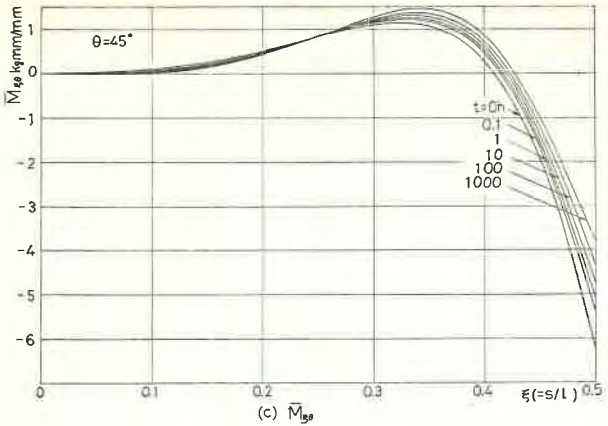

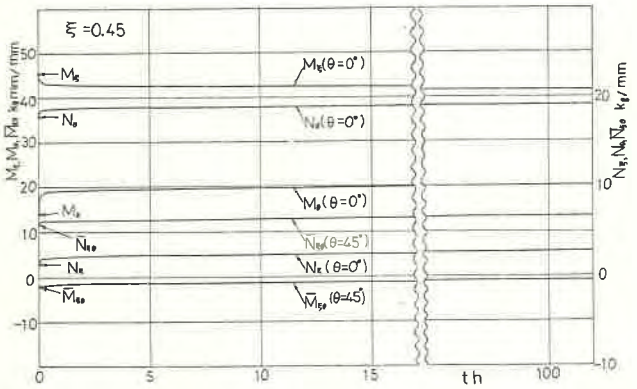

Fig. 10 Variations of internal forces in FG section (ξ =0.45) with time

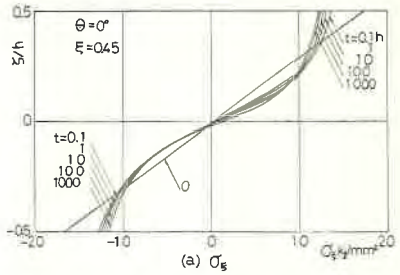

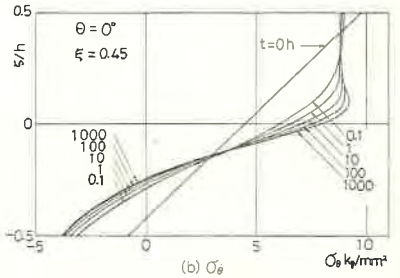

Fig. 9 Stress distributions throuth thickness of shell at point F